

Ambipolar field-effect carrier injections in organic Mott insulatorsT. Hasegawa,^{1,2,*} K. Mattenberger,¹ J. Takeya,^{1,3} and B. Batlogg¹¹Laboratory for Solid State Physics ETH, CH-8093 Zürich, Switzerland²Correlated Electron Research Center, AIST, Tsukuba 305-8562, Japan³Central Research Institute of Electric Power Industry, Komae, Tokyo 201-8511, Japan

(Received 19 December 2003; published 28 June 2004)

We report ambipolar field-effect characteristics observed in metal-insulator-semiconductor field-effect transistor (MISFET) device structures based on organic single crystals of the quasi-one-dimensional (Q1D) Mott-Hubbard insulator (BEDT-TTF)(F₂TCNQ). The main aspects of the measured field-effect properties are well described by the symmetric-gate FET model, which considers the device symmetry of triode FET structures. The temperature-dependent nonlinear nature in the gated-current-voltage characteristics indicates that the ambipolar field-effect carrier injections are present down to 2 K, where the interface barrier potential between the electrode and the Mott insulator appears to be very similar for hole and electron injections, in sharp contrast to the situation involving band insulators.

DOI: 10.1103/PhysRevB.69.245115

PACS number(s): 73.40.Cg, 85.30.Tv, 72.80.Le

I. INTRODUCTION

In the last few years, field-effect doping using metal-insulator-semiconductor field-effect transistor (MISFET) device structures with a variety of materials has attracted considerable attention in materials science.¹⁻⁴ The interests are partly associated with the distinct chemical doping effects in semiconducting materials where the energy gap results from a strong correlation among the electrons.⁵ Transverse field-effect experiments, or field-effect doping, can be a unique tool in condensed matter physics,⁶ and is also expected to produce changes in the materials properties that are of interest for device applications. Here we report unique field-effect characteristics observed in the MISFET device structures based on Mott insulator single crystals of organic charge-transfer (CT) complexes, (BEDT-TTF)(F₂TCNQ) [BEDT-TTF = bis(ethylenedithio)tetrathiafulvalene, F₂TCNQ = 2,5-difluorotetracyanoquinodimethane] (abbreviated hereafter as “ETF2”). It is well known that the family of similar ionic solids opened up vast areas of condensed matter physics, as it produces plenty of organic superconductors.⁷ The CT complexes of ETF2 are composed of 1:1 fully ionized ET⁺¹ cation and F₂⁻¹ anion radicals. It was found from the polarized reflectivity spectra⁸ and intermolecular overlap calculations⁹ that the dominant *side-by-side* intermolecular interaction between ET⁺¹ forms uniform quasi-one-dimensional (Q1D) Mott insulating chains with a CT gap of about 0.7 eV. The neighboring F₂⁻¹ anion radicals on the Mott insulating chains are strongly isolated, showing Curie-like behavior in magnetic susceptibility, followed by an antiferromagnetic (AF) order at around $T_N = 30$ K. The observed magnetic features corroborate that the system are free from periodic lattice distortions (PLD) associated with Peierls or spin-Peierls instabilities along the ET-based Q1D chains down to 2 K.

The observed field-effect characteristics in the ETF2 single crystals presented in this report are found to be ambipolar type, which is preserved down to 2 K. Since any appropriate model has not yet been derived to analyze the am-

bipolar effects that we observed, we establish and utilize a symmetric-gate FET model, in consideration of the device symmetry of triode FET structures. The fundamental field-effect properties are well described by this model. Such ambipolar field-effect characteristics are known to be possible if both types of carriers can be injected into the channel.^{10,11} On the basis of low-temperature current-voltage characteristics the interface carrier injections from metal electrodes into Mott insulators are discussed.

II. PROCEDURES FOR FIELD-EFFECT EXPERIMENTS

The ETF2 single crystals were grown as elongated plates with shiny surfaces with a typical size of $2.5 \times 1 \times 0.2$ mm³. In the crystals, the molecular long axes of ET and F₂ are perpendicular to the plate, and the crystal short axes within the plate are parallel to the Q1D Mott-Hubbard chain. In the fabrication of MISFET device structures, we took particular care, under a microscope, to pick out a flat part of the as-grown crystal surface without bumps and also to avoid mechanical contacts that might damage the crystal surfaces. Gold source and drain contacts (~ 200 nm thick) were deposited on the as-grown crystal surfaces through shadow masks with gaps of 25 μ m. In order not to damage the fragile crystal surfaces, a method was adopted to deposit gate dielectric layers with minimal disturbance of the surfaces: Poly(chloro-*p*-xylylene) (Parylene C) films were fabricated by vapor phase polymerization^{12,13} on top of the crystals. The breakdown field is 2–3 MV/cm (dielectric constant 3.1), at the thickness, about 1.0 μ m. The film thickness was monitored for reference samples simultaneously deposited on glass substrates by a combination of capacitance and optical interference spectrum measurements. Then, the gate electrodes were evaporated on top of the insulators through shadow masks made of pieces of wax papers. The devices that were measured had widths of 300 μ m and a gate dielectric thickness of 1.0 μ m. The electrodes were fabricated to measure the source-drain current along the axis parallel to the Mott insulating chain.

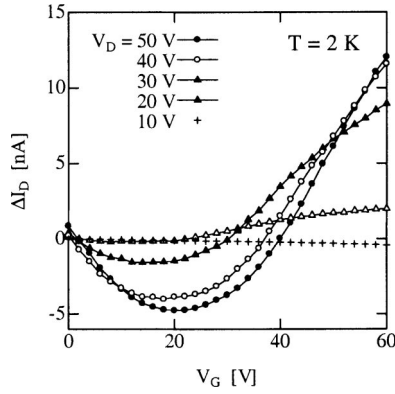


FIG. 1. Transverse field-effect characteristics measured in conventional operation of the MISFET device structures fabricated on an ETF2 single crystal at 2 K. Variation of drain current, ΔI_D , as a function of gate voltage, V_G , at various constant drain voltage, V_D .

We used a combination of two electrometers (Keithley Model 4517A) for the measurements of dc field-effect characteristics. An additional resistor was connected in series with the sample. The voltage drops across the resistor were taken into account to obtain the precise (two contact) field-effect current-voltage characteristics. The sweep of the drain voltage was linked with the gate bias to keep the base of the gate electric potential at half of the drain voltage, as is discussed in Sec. III. In the measurements, the temperature was stabilized within 1 mK to obtain precise field-effect currents.

III. SYMMETRIC GATE OPERATIONS FOR AMBIPOLAR FIELD EFFECTS

In order to establish a simple model for transverse field-effect experiments with the use of MISFET device structures, we first describe the microscopic charge distribution in case that the device allows the accumulation of both positive (p) and negative (n) carriers along the channel (i.e., ambipolar FET).^{2,10,11} Within the “gradual channel approximation,”¹⁴ the charges are accumulated by the potential difference between the gate electrode and the respective position along the channel. For example, when the drain voltage (V_D) is larger than the positive gate bias (V_G), positive carriers are accumulated near the drain electrode in ambipolar FET’s, in sharp contrast to the pinchoff in unipolar FET’s. Consequently, the following puzzling situation occurs in the ambipolar field-effect measurements, if we utilize a conventional procedure: both the polarity and quantity of the total net charge along the channel is not directly associated with V_G , but with the “balance of two variables” as $V_G - V_D/2$. As an example, we show in Fig. 1 the variation of the drain current, ΔI_D , as a function of V_G at various constant V_D , which corresponds to the transfer characteristics of FET’s. In the measurement, the leakage current of the gate bias was much smaller than ΔI_D . We did not observe any noticeable hysteresis in the measurement. We find, upon increasing V_G , that I_D first decreases, reaches a minimum at about $V_G^{\min} \sim V_D/2$, and then increases. The observed minimum clearly originates in the switching of the polarity, from positive to negative, of the total channel charges, as discussed below.

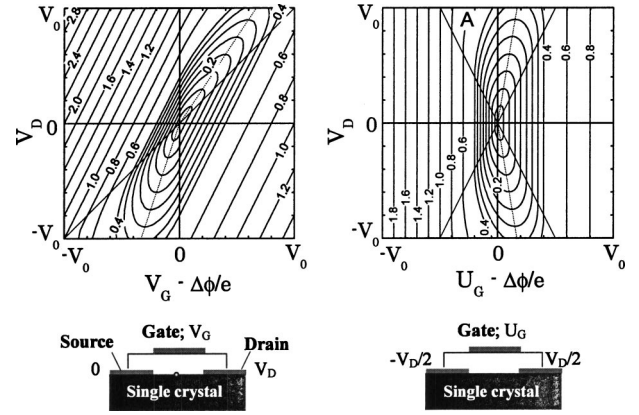


FIG. 2. Calculated contour plot of the channel conductance as a function of drain and gate voltage for an ambipolar FET. (a) Conventional FET operation and (b) symmetric gate operation, which are schematically depicted in the lower panels, respectively.

In order to describe the above features from a theoretical viewpoint, we show in Fig. 2(a) the calculated contour plot of the channel conductance, $\sigma_N(V_G, V_D)$, for ambipolar FET on the basis of the gradual channel approximation.¹⁰ Here the conductivity is plotted in units of $\mu_0 C_i V_0 / 2d$, where C_i is the gate insulator capacitance per unit area and d is the crystal thickness. We assumed undoped intrinsic semiconductor crystals, whose negative and positive carrier mobility is μ_0 and $0.5 \mu_0$, respectively. The dashed line in Fig. 2(a) corresponds to the minima in the V_G dependence of ΔI_D , which very reasonably explains the experimental features shown in Fig. 1. Considering the observed, as well as calculated, results in the ambipolar field effects presented above, we suggest to use “symmetric-gate” operations, in which the electric reference point of the new gate voltage U_G is set at the middle of the source-drain potential [lower panel of Fig. 2(b)], i.e., $U_G = V_G - V_D/2$. In this operation the channel conductance, $\sigma_S(U_G, V_D)$, holds the relation

$$\sigma_S(U_G, V_D) = \sigma_S(U_G, -V_D), \quad (1)$$

reflecting the interchangeable nature between source and drain contacts. In contrast, a similar relation can be obtained in the conventional FET operations,

$$\sigma_N\left(V_G + \frac{V_D}{2}, V_D\right) = \sigma_N\left(V_G - \frac{V_D}{2}, -V_D\right), \quad (2)$$

which is not useful to analyze the ambipolar field effects in which the gate and drain voltage had to be scanned through both polarities. Furthermore, it is found that symmetric-gate operation is very useful to analyze the gated-current-voltage characteristics, as discussed later.

Calculated contour plots of the channel conductance, $\sigma_S(U_G, V_D)$, in the “symmetric-gate” model is shown in Fig. 2(b). We should note that rather large amounts of field-induced charge exist for large $|V_D|$, even at $U_G = 0$, due to the absence of pinchoff that is characteristic of unipolar FET’s. It means that the field-effect current is hard to distinguish from the bulk current. For this reason, we suggest taking the difference between gate-on and gate-off in the field-effect ex-

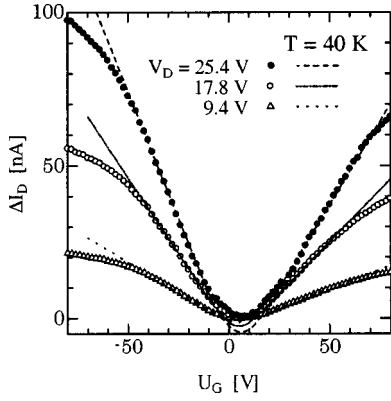


FIG. 3. Transverse field-effect characteristics measured with symmetric-gate operation in the MISFET device structures fabricated on an ETF2 single crystal at 40 K. Variation of drain current, ΔI_D , as a function of symmetric-gate bias, U_G , at various constant drain voltage, V_D . The broken curves are results of a fit according to Eqs. (3)–(5).

periments. We finally give the formulas for the difference $\Delta I_D = I_D(U_G, V_D) - I_D(0, V_D)$ in the respective $V_D - U'_G [V_D > 0]$ regimes¹⁵ (Z and L are channel width and length, respectively):

$$U'_G < -\frac{1}{2}V_D: \quad \Delta I_D = \frac{ZC_i}{2L} \left[-2\mu_p V_D U'_G - \frac{1}{4}(\mu_n + \mu_p)V_D^2 \right], \quad (3)$$

$$-\frac{1}{2}V_D < U'_G < \frac{1}{2}V_D:$$

$$\Delta I_D = \frac{ZC_i}{2L} [(\mu_n + \mu_p)U_G'^2 + (\mu_n - \mu_p)V_D U_G'], \quad (4)$$

$$\frac{1}{2}V_D < U'_G: \quad \Delta I_D = \frac{ZC_i}{2L} \left[2\mu_n V_D U'_G - \frac{1}{4}(\mu_n + \mu_p)V_D^2 \right]. \quad (5)$$

Both positive and negative carriers are accumulated in the region: $-V_D/2 < U'_G < V_D/2$ (U'_G is effective gate bias $U_G - \Delta\phi$), while the channel includes only positive carriers for $U'_G < -V_D/2$ and negative carriers in the region $V_D/2 < U'_G$.

IV. FUNDAMENTAL FIELD-EFFECT CHARACTERISTICS

We show in Fig. 3 the measured field-effect characteristics of an ETF2 single crystal; the change of the drain current ΔI_D , in response to an applied gate bias U_G at constant V_D , using the symmetric-gate operation at 40 K. The broken curves are the results of a fit according to Eqs. (3)–(5). The observed ΔI_D was several percent of the I_D . The ΔI_D exhibits clear enhancement by the application of both positive and negative U_G , providing unambiguous evidence of the ambipolar field effect. It is noted that the observed persistent ambipolar-type enhancement cannot be understood by assuming any set of charged impurities, considering that the applied transverse electric field on the crystal surface should

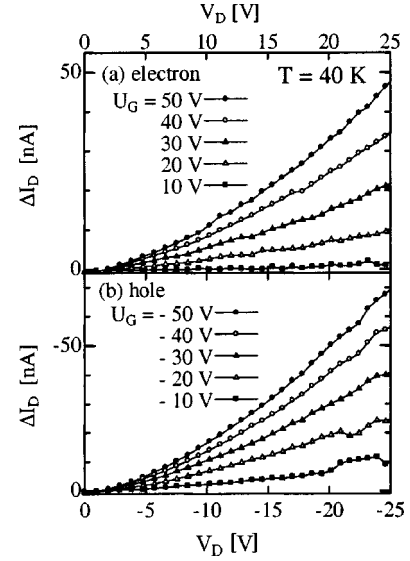


FIG. 4. Gated-current-voltage [$\Delta I_D - V_D; \Delta I_D = \Delta I_D(U_G, V_D) - \Delta I_D(0, V_D)$] characteristics at various symmetric-gate bias, U_G , in the MISFET device structures based on an ETF2 single crystal at 40K for (a) electron and (b) hole doping operations.

terminate at the insulator-semiconductor interface in the range of the Thomas-Fermi screening length, as long as the carriers are persistently injected from the electrodes. The results clearly show that both p - and n -type carriers can be injected from Au electrodes into the channel. The observed curves exhibit slightly larger increasing rates at negative U_G , indicating that μ_p is larger than μ_n . The overall features of the experimental results are well reproduced by the theoretical curves. The carrier density is estimated as $8.7 \times 10^{-5}/\text{\AA}^2$ at $U'_G = 50$ V, implying that the carrier number per molecule is at most 0.4%. The fitting results also imply that the U_G^{\min} is slightly larger (by about 2–3 V) than expected if one considers the ratio μ_p/μ_n and the $\Delta\phi$ of about 1 eV.¹⁶ We conjecture that the crystal might be weakly p doped, which is depleted by the small positive U_G and effects the shift of U_G^{\min} ,¹⁰ although the origin of such trace amounts of charged impurities is difficult to be investigated. Near the minimum, slight deviations are also observed between calculated and measured values in the region $|U'_G| < V_D/2$, where both types of carriers are accumulated. We expect that the carrier transport would be more efficient than expected, due to the electron-hole recombination within the channel, assuming independent current flow of the respective carriers.

We estimate the field-effect mobility from the slopes of the curves in the regions, $|U'_G| > |V_D|/2$. We note that the estimate is essentially the same as in the linear regions of unipolar FET's. We find that μ_p and μ_n depend on V_D ; The values at $T = 40$ K are $\mu_p = 0.00194 \text{ cm}^2/Vs$ and $\mu_n = 0.00128 \text{ cm}^2/Vs$ ($V_D = 25.4$ V), 0.00167 and 0.00114 cm^2/Vs ($V_D = 17.8$ V), and 0.00126 and 0.00080 cm^2/Vs ($V_D = 9.4$ V), respectively. Importantly, the ratio μ_p/μ_n is constant at about 1.5, independent of V_D . In Fig. 4, we show the gated-current-voltage characteristics ($\Delta I_D - V_D$) at 40 K, at various gate voltages U_G for n -type (upper) and p -type (lower) operations. It is found that the observed

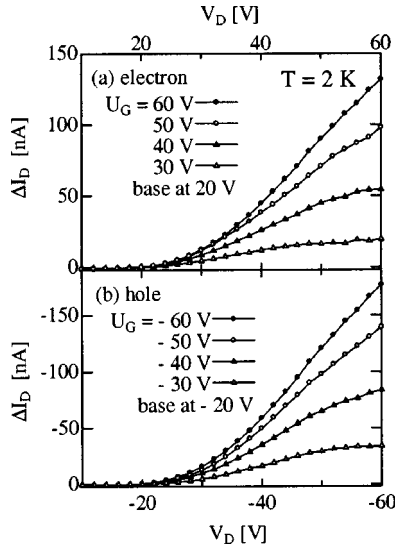


FIG. 5. Gated-current-voltage (ΔI_D - V_D) characteristics at various symmetric-gate bias, U_G , in the MISFET device structures based on ETF2 single crystal at 2 K for (a) electron and (b) hole doping operations. The reference gate voltage for the drain current is set at 20 V [(a) $\Delta I_D = \Delta I_D(U_G, V_D) - \Delta I_D(20 \text{ V}, V_D)$], and at -20 V [(b) $\Delta I_D = \Delta I_D(U_G, V_D) - \Delta I_D(-20 \text{ V}, V_D)$], respectively, due to the observed negative features at lower V_D range, if we use $U_G = 0 \text{ V}$ as the reference (Fig. 7).

ΔI_D - V_D curves are superlinear for both operations, in contrast to Eqs. (3) and (5), which predict convex upward in the regions $|V_D|/2 < |U'_G|$. This discrepancy should be associated with the nonlinear nature of the ΔI_D - V_D characteristics, which is also the origin of the V_D -dependent field-effect mobility, as denoted above. In Fig. 5, we show the similar ΔI_D - V_D curves at 2 K. The nonlinearity becomes more remarkable in the low V_D range at 2 K. The temperature-dependent nonlinear nature in the ΔI_D - V_D characteristics will be discussed further in Sec. IV. We also notice from the curves at $U_G = 30 \text{ V}$ and $U_G = -30 \text{ V}$ in Fig. 5, that $d(\Delta I_D)/dV_D$ decreases gradually in the high V_D range above 50 V, which seems to be similar to the current saturation in the I_D - V_D characteristics of unipolar FET's. This feature can be ascribed to the saturation in the ΔI_D - V_D characteristics in the case of $\mu_p \sim \mu_n$, as predicted by Eq. (4).

From the analyses of the ΔI_D - U_G characteristics at various temperatures, we extract the temperature dependence of the field-effect mobility. We find that the ratio μ_p/μ_n remains about 1.5 for all the measured temperature range (2–60 K), so that the temperature-dependent features are almost the same for p - and n -type operations. The result is shown in Fig. 6 for μ_p . Because of the nonlinearity in the ΔI_D - V_D characteristics, the discrepancy between $V_D \sim 60$ and $\sim 30 \text{ V}$ becomes large at low temperature. The important observation is that the mobility (estimated at $V_D \sim 60 \text{ V}$) increases as the temperature decreases at least above 10 K. This feature should be associated with the decrease of the electron-phonon scattering rate as temperature decreases. This might be taken as evidence for coherent band transport, although the measured mobility values are very low.

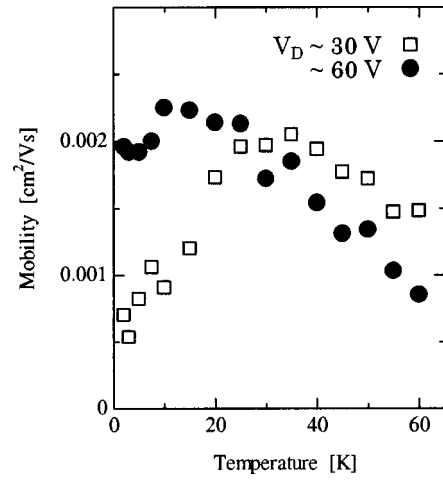


FIG. 6. Temperature dependence of field-effect hole mobility in the MISFET device structures based on ETF2 single crystal measured at $V_D \sim 30 \text{ V}$ (open squares) and $V_D \sim 60 \text{ V}$ (filled circles).

V. AMBIPOLAR CARRIER INJECTIONS IN ORGANIC MOTT INSULATORS

From the observations described above, it is concluded that the ambipolar field-effects in ETF2 single crystal are essentially independent of the temperature down to 2 K, even though the nonlinearity in the ΔI_D - V_D characteristics becomes more prominent at lower temperature. To discuss the origin of the nonlinearity, we show in Fig. 7, for comparison, the current-voltage (I_D - V_D , left-hand side) and gated-current-voltage (ΔI_D - V_D , middle for p -type and right-hand side for n -type) characteristics. The nonlinearity in the ΔI_D - V_D characteristics becomes more and more pronounced as the temperature decreases. It is also important to point out that the nonlinear features seem to be similar for p - and n -type operations at respective temperatures.

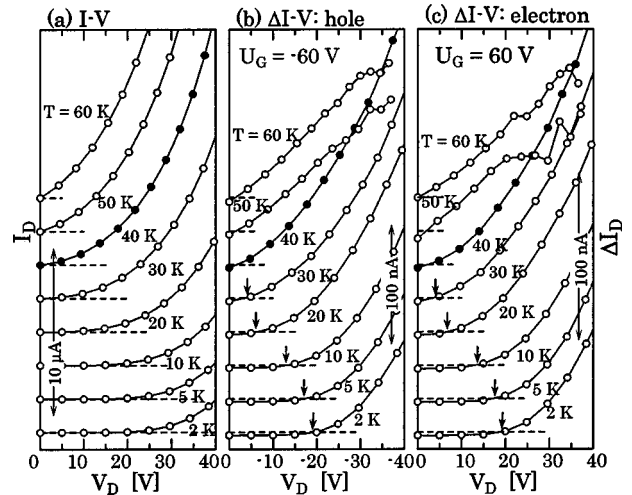


FIG. 7. Conventional (two Au contacts) current-voltage (I_D - V_D) characteristics at $U_G = 0 \text{ V}$ (left), gated-current-voltage (ΔI_D - V_D) characteristics for p type [middle: $\Delta I_D = I_D(-60 \text{ V}, V_D) - I_D(0, V_D)$] and n type [right: $\Delta I_D = I_D(60 \text{ V}, V_D) - I_D(0, V_D)$] in the MISFET device structures based on an ETF2 single crystal at various temperatures. Arrows indicate the sign change of ΔI_D .

It is also seen from Fig. 7 that the nonlinear ΔI_D - V_D characteristics appear to reflect the nonlinear nature of the bulk I_D - V_D characteristics. In the high V_D range, this nonlinearity might be associated with the space-charge-limited current or the emission-limited current, as observed in a number of organic semiconducting materials.¹⁷ Rather, it is also probable that the observed nonlinearity should be associated with the unique features of nonlinear carrier transport in organic Mott insulators.¹⁸ Meanwhile, the ΔI_D is observed to become negative, e.g., $V_D < 20$ V at 2 K in Fig. 7, as shown by the arrows, which can be regarded as clear evidence of the interface barrier potential effect against carrier injections in the low V_D range. Carriers are difficult to inject into the crystals at low V_D , so the gate fields will not terminate at the insulator-semiconductor interface but will penetrate into the semiconductor. Consequently, additional longitudinal fields are generated near the drain electrode, with the sign opposite to the source-drain field, and can generate the negative sign of ΔI_D . The similarity in the ΔI_D - V_D characteristics, in the low V_D range, most likely indicates that both p - and n -type carrier injections are determined by a very similar interface barrier potential. The important observation is that the injection of holes and electrons is almost equally possible down to 2 K, in spite of the observed nonlinear nature, which is in sharp contrast to the situation in conventional metal-semiconductor interfaces.

Notwithstanding a desire for ambipolar MISFET's, which would enable highly accumulated low-power logic circuits with a single active material, it is known that in conventional FET's a severe difficulty is encountered in the interface carrier injection at the source and drain contacts. In organic materials, it is usually observed that a good ohmic contact for one carrier type tends to block the charge carriers of opposite sign, in spite of the low density of the surface states in the van der Waals-type bonded molecular crystals. These features originate in the general feature of metal-semiconductor interfaces that are asymmetric with respect to p - and n -type carrier injections, because of the band gap.¹⁹ Actually, conventional organic thin film transistors (OTFT's) are a unipolar device, either p or n type.¹ This feature is also used as a built-in technology in the organic light emitting diodes (OLED's).²⁰ We suggest that the present observation of ambipolar carrier injections down to 2 K to be characteristic for the Mott insulators, where both holes and electrons are associated with an identical band.

To speculate on the microscopic mechanism, an analogy to the best studied doped Mott system, i.e., the high- T_C cuprates, might be helpful; it has been known that the resistivity diminishes with decreasing temperature over a wide temperature range above ~ 50 K, even for compounds with carrier concentrations as low as $\sim 1\%$, though the value of resistivity is extraordinarily large.²¹ Since the mean free path would be too short for the "metal" with homogeneous charge density, it is argued that the charges are inhomogeneously

distributed due to the strong electron-electron correlation.²² Recently it has been suggested, based both on experimental and theoretical grounds, that the regions with high carrier density, responsible for the "metallic" resistivity, are segregated from insulating regions with antiferromagnetically interacting localized spins.²³ Provided that the phase separation takes place similarly in the organic Mott insulators, one can expect ohmic contacts from the "metallic" segments in the active material to the electrodes only when the charges are injected, which would enable the ambipolar operations. It is also noteworthy that the mobility increases with decreasing temperature at least above 10 K at $V_D \sim 60$ V, as described above, and is typical for coherent bandlike transport. The absolute value of μ_p and μ_n , however, appears inconsistent with the coherent band transport by several orders of magnitude. The assumption of a filamentary conduction is also appealing to reconcile this apparent contradiction, as has been discussed for the high- T_C cuprates. It might be useful for further investigations to measure the temperature dependence of the bulk mobility by time-of-flight technique on the organic Mott insulators. All these findings on the interface charge transport, as well as the nonlinear carrier transport, may well represent a particular aspect of the Mott insulators that should be investigated in detail from both experimental and theoretical viewpoints.

VI. CONCLUSIONS

We succeeded in the observation of ambipolar transverse field effects in the MISFET device structures, based on single crystals of Q1D Mott insulator ETF2. The symmetric-gate ambipolar FET model affords a comprehensive description of the observed ambipolar field-effect characteristics. From the low temperature field-effect features it is concluded that ambipolar carrier injection can be achieved down to 2 K. The nonlinear nature in the gated-current-voltage characteristics suggests that the interface barrier potential is about the same for hole and electron injections into the Mott insulator. The hole mobility is ~ 1.5 times larger than the electron mobility and increases upon cooling between ~ 60 and 10 K. This could be taken as evidence for coherent band transport, except that the measured mobility values are too low by some three orders of magnitude. This raises the question about possible microscopic distribution of the charge that is field-effect induced into this Mott insulator with large electron correlations.

ACKNOWLEDGMENTS

This study was supported by the Swiss National Science Foundation. T.H. also acknowledges an overseas research program, dispatched from the Research Institute for Electronic Science in Hokkaido University and administered by the Ministry of Education, Culture, Science, and Technology (MEXT) of Japan.

*Electronic address: t-hasegawa@aist.go.jp

- ¹C. D. Dimitrakopoulos and P. R. L. Malenfant, *Adv. Mater.* (Weinheim, Ger.) **14**, 99 (2002).
- ²A. Bachtold, P. Hadley, T. Nakanishi, and C. Dekker, *Science* **294**, 1317 (2001).
- ³N. Stutzmann, R. H. Friend, and H. Sirringhaus, *Science* **299**, 1881 (2003).
- ⁴C. H. Ahn, J.-M. Triscone, and J. Mannhart, *Nature* (London) **424**, 1015 (2003).
- ⁵M. Imada, A. Fujimori, and Y. Tokura, *Rev. Mod. Phys.* **70**, 1039 (1998).
- ⁶E. Abrahams, S. V. Kravchenko, and M. P. Sarachik, *Rev. Mod. Phys.* **73**, 251 (2001).
- ⁷T. Ishiguro, K. Yamaji, and G. Saito, *Organic Superconductors*, 2nd ed. (Springer-Verlag, Berlin, 1998).
- ⁸T. Hasegawa, S. Kagoshima, T. Mochida, S. Sugiura, and Y. Iwasa, *Solid State Commun.* **103**, 489 (1997).
- ⁹T. Hasegawa, T. Mochida, R. Kondo, S. Kagoshima, Y. Iwasa, T. Akutagawa, T. Nakamura, and G. Saito, *Phys. Rev. B* **62**, 10059 (2000).
- ¹⁰H. Pfeleiderer, *IEEE Trans. Electron Devices* **ED-33**, 145 (1986).
- ¹¹G. W. Neudeck, H. F. Bare, and K. Y. Chung, *IEEE Trans. Electron Devices* **ED-34**, 344 (1987).
- ¹²C. D. Dimitrakopoulos and D. J. Mascaró, *IBM J. Res. Dev.* **45**, 11 (2001).
- ¹³V. Podzorov, V. M. Pudalov, and M. E. Gershenson, *Appl. Phys. Lett.* **82**, 1739 (2003).
- ¹⁴S. M. Sze, *Physics of Semiconductor Devices*, 2nd ed. (Wiley, New York, 1981).
- ¹⁵The expressions can be derived from the modifications of the ambipolar FET Eqs. (8) and (9) in Ref. 10.
- ¹⁶N. Sato, G. Saito, and H. Inokuchi, *Chem. Phys.* **76**, 79 (1983).
- ¹⁷M. Pope and C. E. Swenberg, *Electronic Processes in Organic Crystals and Polymers*, 2nd ed. (Oxford University Press, New York, 1999), Chap. XIV.
- ¹⁸R. Kumai, Y. Okimoto, and Y. Tokura, *Science* **284**, 1645 (1999).
- ¹⁹K. H. Heinz, *Semiconductor Contacts: An Approach to Ideas and Models* (Clarendon, Oxford, 1994).
- ²⁰C. W. Tang and S. A. VanSlyke, *Appl. Phys. Lett.* **51**, 913 (1987).
- ²¹H. Takagi, T. Ido, S. Ishibashi, M. Uota, S. Uchida, and Y. Tokura, *Phys. Rev. B* **40**, 2254 (1989).
- ²²Y. Ando, A. N. Lavrov, S. Komiya, K. Segawa, and X. F. Sun, *Phys. Rev. Lett.* **87**, 017001 (2001).
- ²³E. W. Carlson, S. A. Kivelson, and D. Orgad, cond-mat/0206217 (unpublished).